Electronic Supporting Information

A luminescent G-quadruplex switch-on probe for the highly selective and tunable detection of cysteine and glutathione†

Ka-Ho Leung,[a] Hong-Zhang He,[a] Victor Pui-Yan Ma,[a] Daniel Shiu-Hin Chan,[a] Chung-Hang Leung*[b] and Dik-Lung Ma*[a]

[a] *Department of Chemistry, Hong Kong Baptist University, Kowloon Tong, Hong Kong, China.*
E-mail: edmondma@hkbu.edu.hk
[b] *State Key Laboratory of Quality Research in Chinese Medicine, Institute of Chinese Medical Sciences, University of Macau, Macao, China*
E-mail: duncanleung@umac.mo

Experimental section

Materials. Reagents were purchased from Sigma Aldrich (St. Louis, MO) and used as received. Iridium chloride hydrate ($IrCl_3.xH_2O$) was purchased from Precious Metals Online (Australia). All oligonucleotides were synthesized by Techdragon Inc. (Hong Kong, China).

DNA sequences:

	Sequence
PS2.M	5′-$GTG_3TAG_3CG_3T_2G_2$-3′
ss DNA	5′-$CTCAT_4C_2ATACAT_2A_3GATAGTCAT$-3′
Pu22	5′-$TGAG_3TG_4AG_3TG_4A_2$-3′
Pu27	5′-$TG_4AG_3TG_4AG_3TG_4A_2G_2$-3′

General experimental. Mass spectrometry was performed at the Mass Spectroscopy Unit at the Department of Chemistry, Hong Kong Baptist University, Hong Kong (China). Melting points were determined using a Gallenkamp melting apparatus and are uncorrected. Deuterated solvents for NMR purposes were obtained from Armar and used as received.

^1H and ^{13}C NMR were recorded on a Bruker Avance 400 spectrometer operating at 400 MHz (^1H) and 100 MHz (^{13}C). ^1H and ^{13}C chemical shifts were referenced internally to solvent shift (CD_3CN: ^1H, δ 1.94, ^{13}C δ 118.7; d_6-DMSO: ^1H δ 2.50, ^{13}C δ 39.5). Chemical shifts (δ) are quoted in ppm, the downfield direction being defined as positive. Uncertainties in chemical shifts are typically ±0.01 ppm for ^1H and ±0.05 for ^{13}C. Coupling constants are typically ± 0.1 Hz for ^1H-^1H and ±0.5 Hz for ^1H-^{13}C couplings. The following abbreviations are used for convenience in reporting the multiplicity of NMR resonances: s, singlet; d, doublet; t, triplet; q, quartet; m, multiplet; br, broad. All NMR data was acquired and processed using standard Bruker software (Topspin).

Photophysical measurement. Emission spectra and lifetime measurements for complex **1** were performed on a PTI TimeMaster C720 Spectrometer (Nitrogen laser: pulse output 337 nm) fitted with a 380 nm filter. Error limits were estimated: λ (±1 nm); τ (±10%); φ (±10%). All solvents used for the lifetime measurements were degassed using three cycles of freeze-vac-thaw.

Luminescence quantum yields were determined using the method of Demas and Crosby[1] $[Ru(bpy)_3][PF_6]_2$ in degassed acetonitrile as a standard reference solution ($\Phi_r = 0.062$) and calculated according to the following equation:

$$\Phi_s = \Phi_r(B_r/B_s)(n_s/n_r)^2(D_s/D_r)$$

where the subscripts s and r refer to sample and reference standard solution respectively, n is the refractive index of the solvents, D is the integrated intensity, and Φ is the luminescence quantum yield. The quantity B was calculated by $B = 1 - 10^{-AL}$, where A is the absorbance at the excitation wavelength and L is the optical path length.

Synthesis

The following compounds were prepared according to the reported literature method, the precursor complex $[Ir_2(phq)_4Cl_2]$,[2] and 2,9-diphenyl-1,10-phenanthroline (dpp)[3] are characterized by ^{1}H-NMR,^{13}C-NMR and High Resolution Mass Spectrometry (HRMS).

$[Ir(phq)_2(dpp)]PF_6$ (1). A suspension of $[Ir_2(phq)_4Cl_2]$ (0.2 mmol) and 2,9-diphenyl-1,10-phenanthroline (0.44 mmol) in a mixture of DCM:methanol (1:1, 20 mL) was refluxed overnight under a ntirogen atmosphere. The resulting solution was then allowed to cool to room temperature, and filtered to remove unreacted cyclometallated dimer. To the filtrate, an aqueous solution of ammonium hexafluorophosphate (excess) was added and the filtrate was reduced in volume by rotary evaoration until precipitation of the crude product occurred. The precipiate was then filtered and washed with several portions of water (2 × 50 mL) followed by diethyl ether (2 × 50 mL). The product was recrystallized by acetonitrile:diethyl ether vapor diffusion to yield the titled compound as a red-orange solid.

Yield: 76%. ^{1}H NMR (400 MHz, CD_3CN) d 8.51 (d, J = 8.0 Hz, 2H), 8.21 (d, J = 8.0 Hz, 2H), 7.85–7.81 (m, 6H), 7.69 (d, J = 8.0 Hz, 2H), 7.54 (d, J = 8.0Hz, 2H), 7.4–7.32 (m, 4H), 7.06 (t, J = 8.0 Hz, 2H), 6.95–6.91 (m, 2H), 6.62 (t, J = 8.0 Hz, 2H), 6.53–6.48 (m, 8H), 6.22 (t, J = 8.0 Hz, 2H), 5.75 (d, J = 8.0Hz, 2H); ^{13}C NMR (400 MHz, CD_3CN) d 172.7, 165.8, 150.2, 148.9,148.8, 146.1, 140.6, 139.9, 139.7, 134.1, 131.8, 131.7, 131.2, 130.5, 130.1, 129.6, 129.0, 128.8, 128.7, 128.5, 128.2, 127.6, 125.6, 123.0; MALDI-TOF-HRMS: Calcd. for $C_{54}H_{36}IrN_4$ $[M–PF_6]^+$: 933.2567 Found: 933.2506.

Emission response of 1 towards different forms of DNA

The G-quadruplex DNA-forming sequences (PS2.M, Pu22 and Pu27) were annealed in Tris-HCl buffer (20 mM Tris, 100 mM KCl, pH 7.0) and were stored at –20 °C before use. Complex **1** (1 μM) was added to 5 μM of ss DNA, ct DNA or G-quadruplex DNA in Tris-HCl buffer (20 mM Tris, pH 7.0) containing. Emission spectra were recorded in 550−750 nm range using an excitation wavelength of 360 nm.

Emission titration for the detection of cysteine and glutathione in buffered solution

The PS2.M DNA (100 μM) was first annealed in Tris-HCl buffer (20 mM Tris, 100 mM KCl, pH 7.0). The solution was heated to 95 °C for 10 min and then cooled to room temperature at 0.1 ^{o}C/s to ensure formation of the PS2.M G-quadruplex. The annealed product was stored at –20 °C before use. A solution containing complex 1 (1 μM), pre-annealed PS2.M G-quadruplex (5 μM) and the indicated concentration of Hg^{2+} were incubated at 25 °C for 3 h in Tris-HCl buffer (20 mM Tris, pH 7.0). Aliquots of cysteine (0–40 μM) or glutathione (0–19 μM) were added to the buffered solution. Emission spectra were recorded in the 500−690 nm range using an excitation wavelength of 360 nm. The selectivity assay was performed

using a similar protocol except that a ten-fold excess of other amino acids (5, 10 and 15 μM) was used compare to cysteine and glutathione (0.5, 1.0 and 1.5 μM) were used.

Fig. S1 UV/vis absorption and normalized emission spectra of complex **1** (20 μM) in acetonitrile solution at 298K.

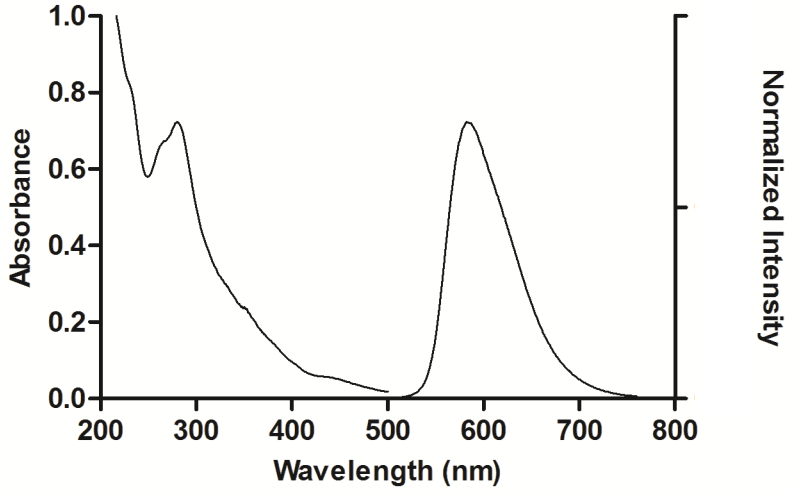

Fig. S2 Emission spectra of complex **1** (solid line) and the reference complex $[Ru(bpy)_3]^{2+}$ (dotted line) in acetonitrile solution at 298K.

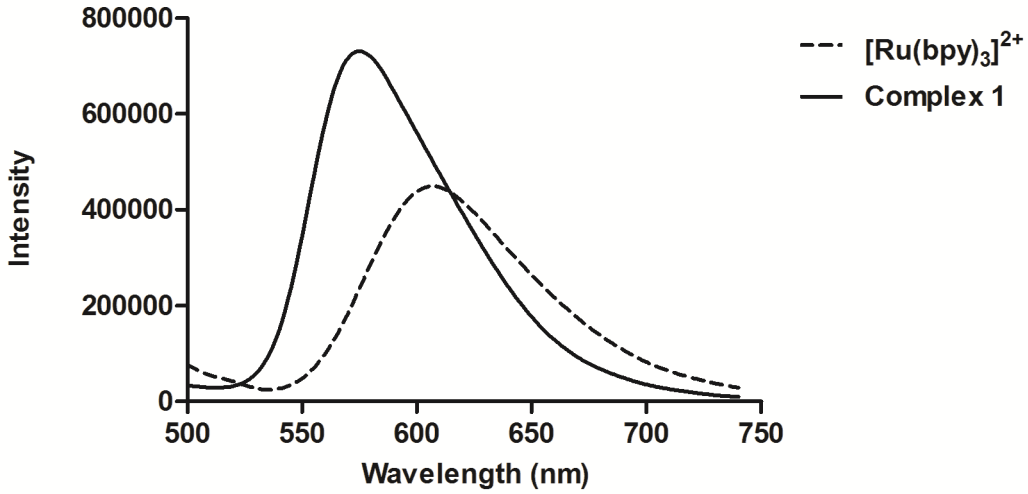

Fig. S3 Emission spectrum of complex **1** (1 μM) in the presence of 5 μM of ss DNA, ct DNA or various G-quadruplexes.

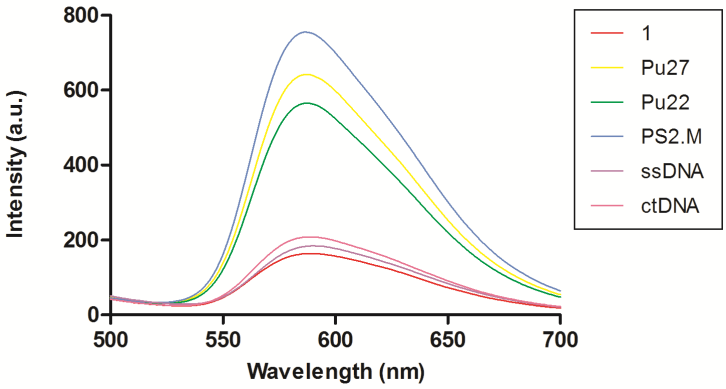

Fig. S4 Stern-Volmer plot (I_0 / I) of the **1**/G-quadruplex ensemble in the presence of (A) 0.5 μM, (B) 5 μM, (C) 10 μM, (D) 100 μM, (E) 500 μM and (F) 1000 μM Hg^{2+} at λ = 583 nm *vs.* Cys concentration. Error bars represent the standard deviations of the results from three independent experiments.

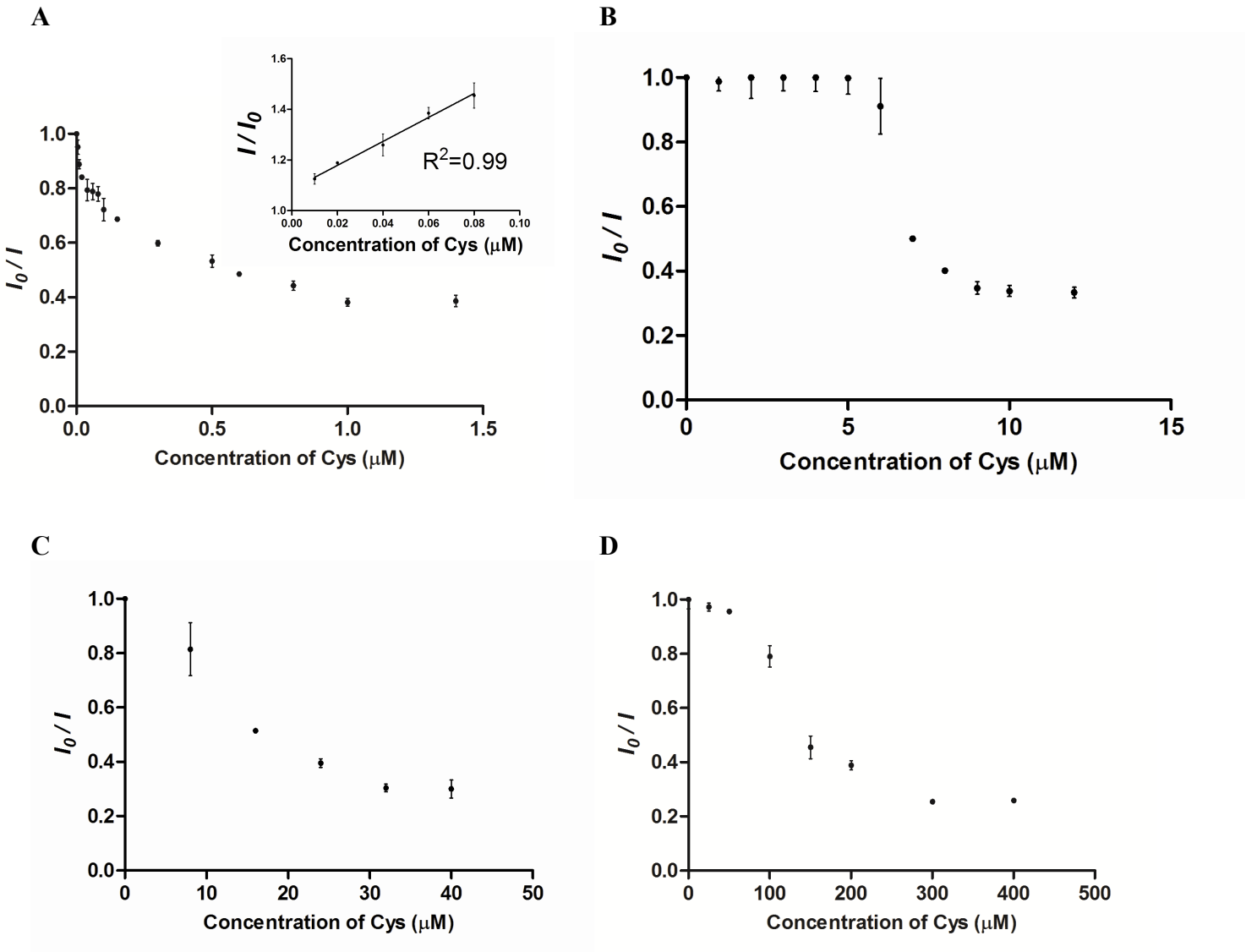

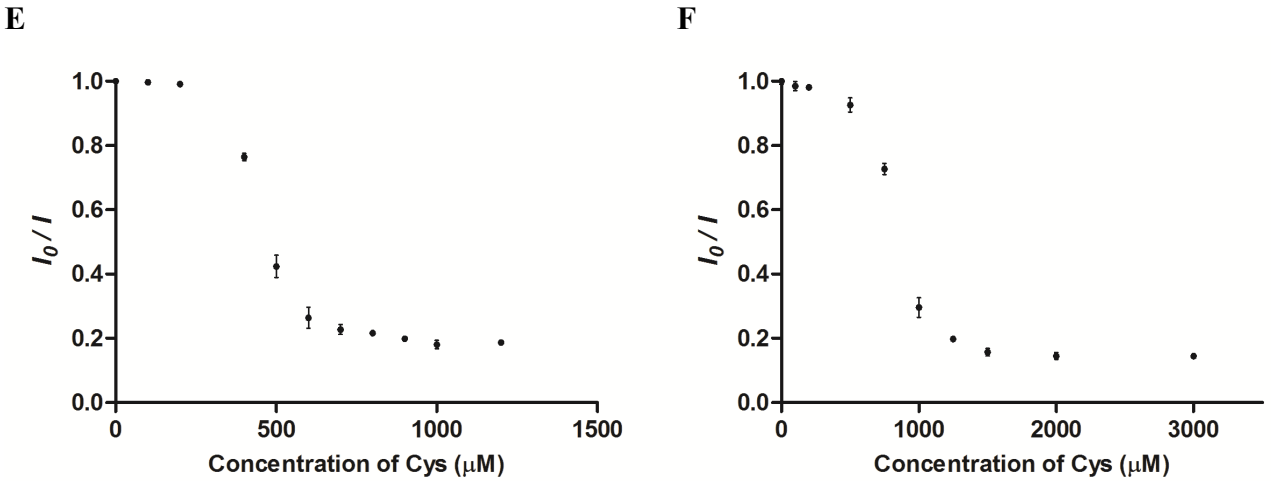

Fig. S5 Emission spectral traces of of the **1**/G-quadruplex/Hg^{2+} ensemble ([**1**] = 1 μM, [PS2.M] = 5 μM, [Hg^{2+}] = 0.5 μM) in the presence of (A) 0, 5 and 10 nM Cys, (B) 0 and 10 nM GSH, showing a signal-to-noise ratio greater than 3.

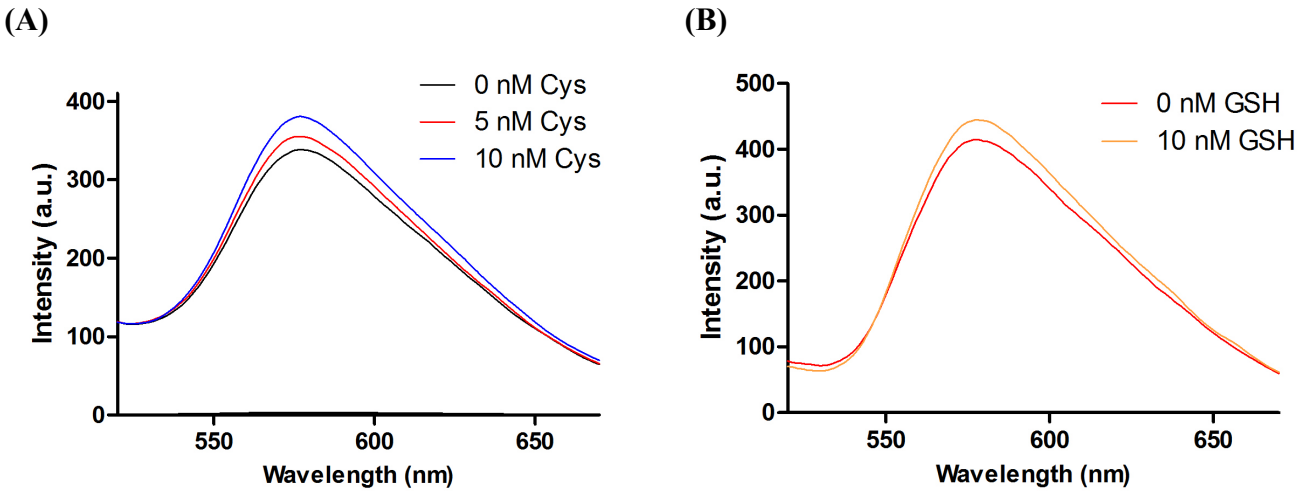

Fig. S6 Photograph image of the **1**/G-quadruplex/Hg^{2+} ensemble (1 μM of **1**, 5 μM of PS2.M, 1 μM of Hg^{2+}) in Tris buffer (20 mM, pH 7.0) in the presence (left) or absence (right) of 2 μM cysteine.

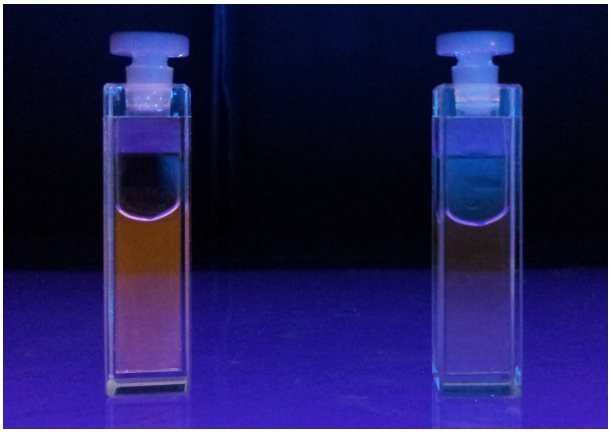

Fig. S7 Time course of luminescence response of the **1**/G-quadruplex/Hg^{2+} ensemble ([**1**] = 1 μM; [PS2.M] = 5 μM; [Hg^{2+}] = 1 μM) in the presence of 1 μM Cys or GSH.

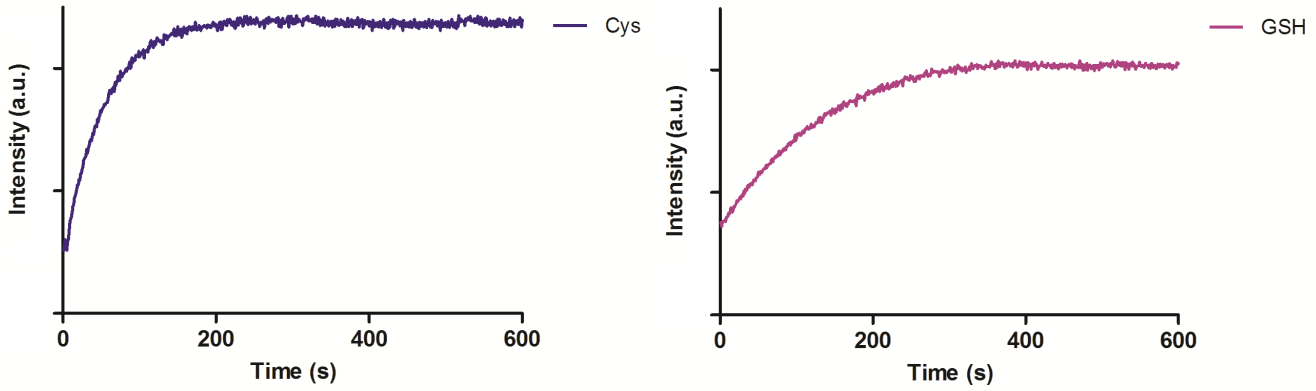

Fig. S8 Stern-Volmer plot of the **1**/G-quadruplex ensemble ([**1**] = 1 μM; [PS2.M] = 5 μM; [Hg^{2+}] = 500 μM) in the presence of (A) increasing ratio of GSH/GSSG; (B) increasing ratio of Cys/Cys-Cys; (C) change of luminescence intensity of the three component ensemble ([**1**] = 1 μM; [PS2.M] = 5 μM; [Hg^{2+}] = 500 μM) in the presence of 500 μM Cys, GSH, Cys-Cys or GSSG. Error bars represent the standard deviations of the results from three independent experiments.

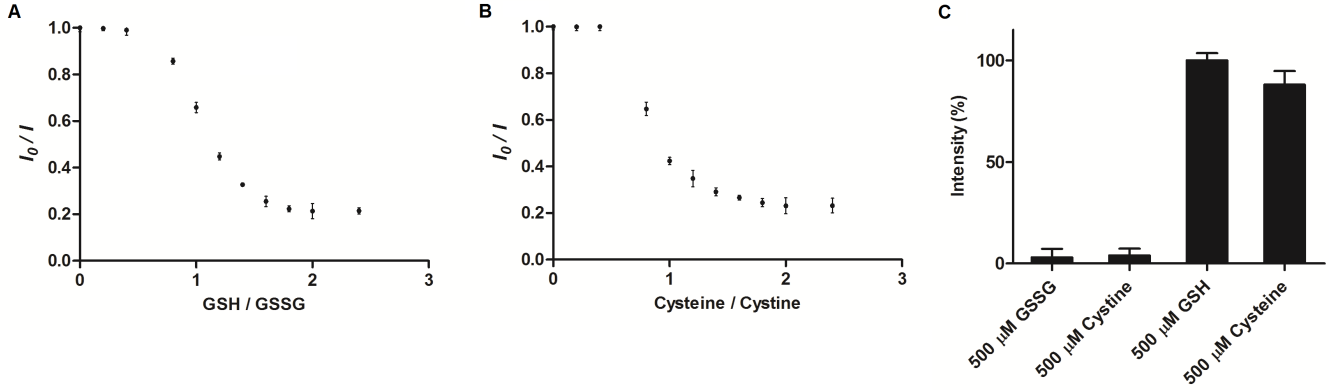

Fig. S9 Relative luminescence intensity of the **1**/G-quadruplex ensemble ([**1**] = 1 μM; [PS2.M] = 5 μM) with or without 1 μM Hg^{2+} ions in the presence of increasing concentrations of Cys (0, 0.25, 0.5, 1, 1.5, 2, 2.5 and 3 μM).

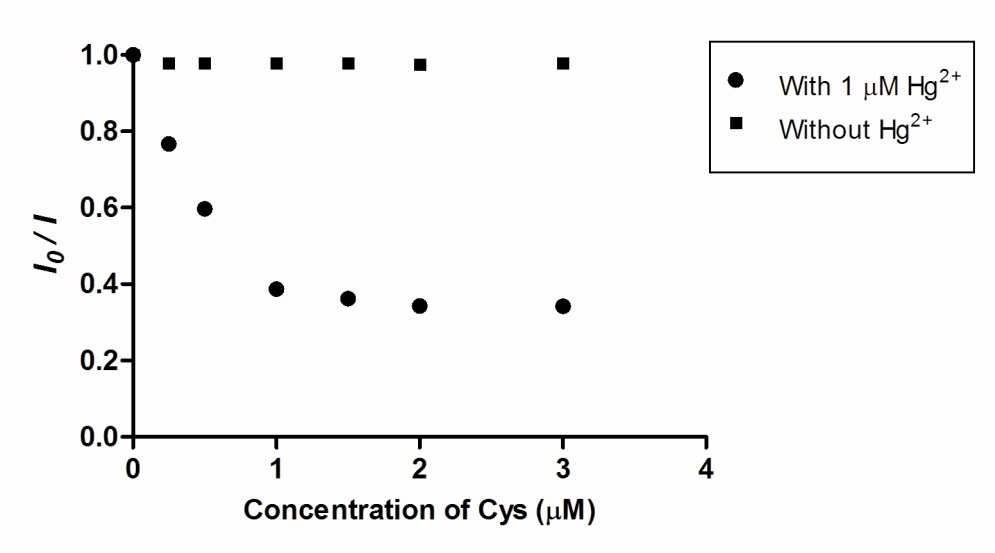

Fig. S10 Stern-Volmer plot (I_0 / I) of the **1**/G-quadruplex ensemble in the presence of (A) 0.5 μM, (B) 1 μM, (C) 5 μM, (D) 10 μM, (E) 100 μM, (F) 500 μM and (G) 1000 μM Hg^{2+} at λ = 583 nm *vs.* GSH concentration. Inset: linear plot of the change in luminescence intensity at λ = 583 nm *vs.* GSH concentration.

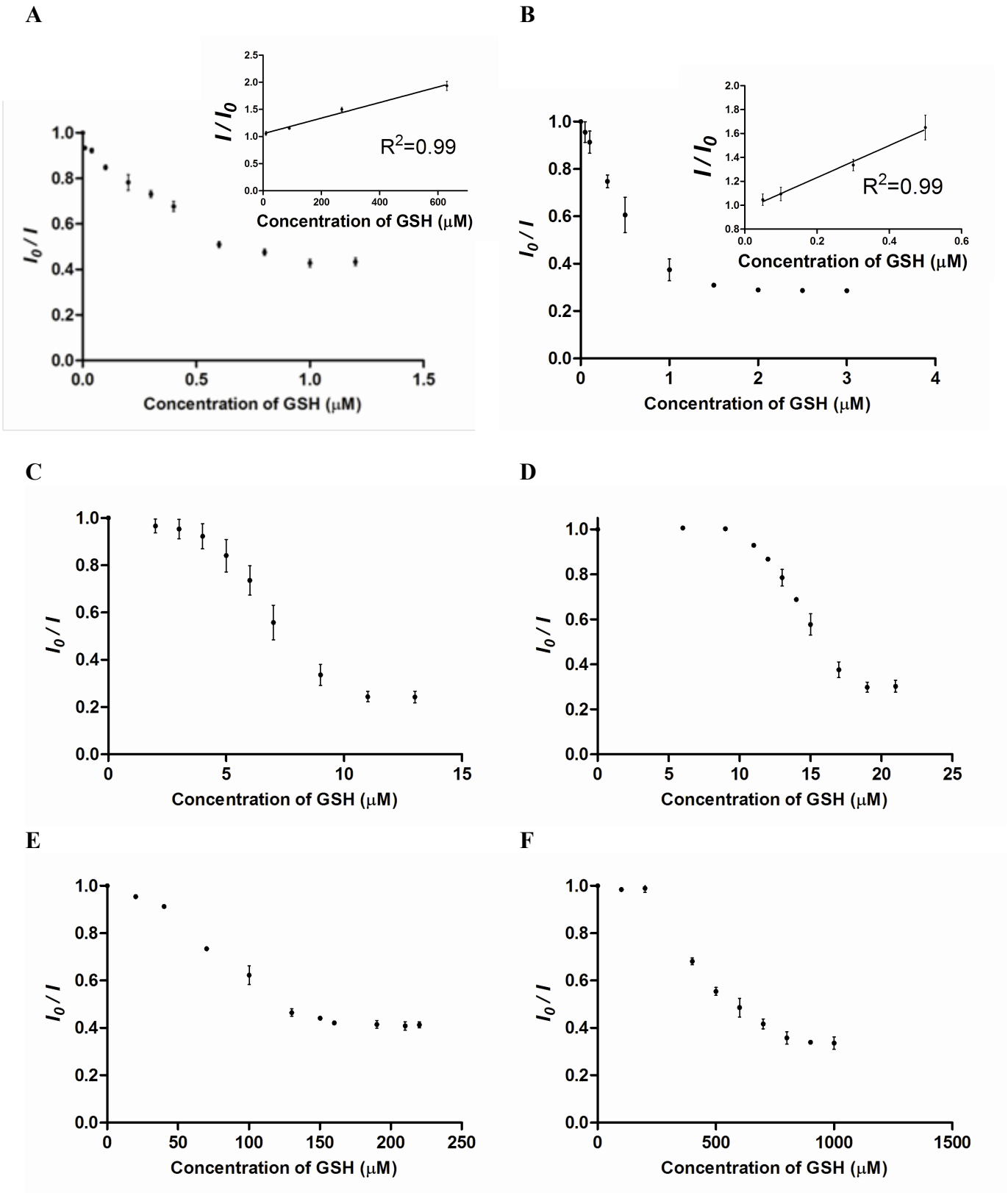

G

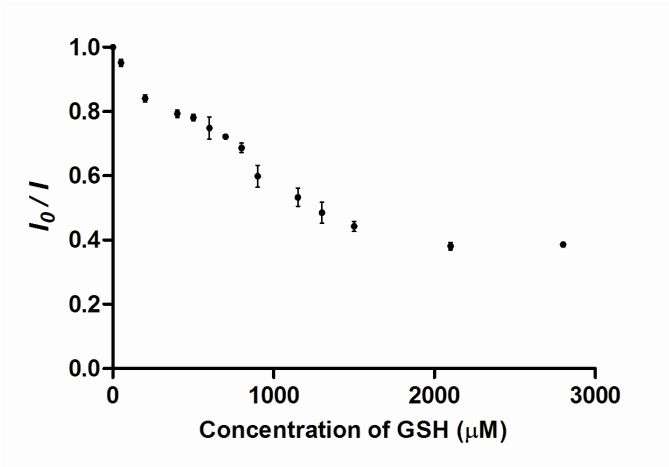

Fig. S11 Relative luminescence intensity of **1**/G-quadruplex ensemble ([**1**] = 1 μM; [PS2.M] = 5 μM) in the presence or absence of 1 μM Hg^{2+} ions in the presence of increasing concentrations of GSH (0, 0.25, 0.5, 1, 1.5 and 2 μM).

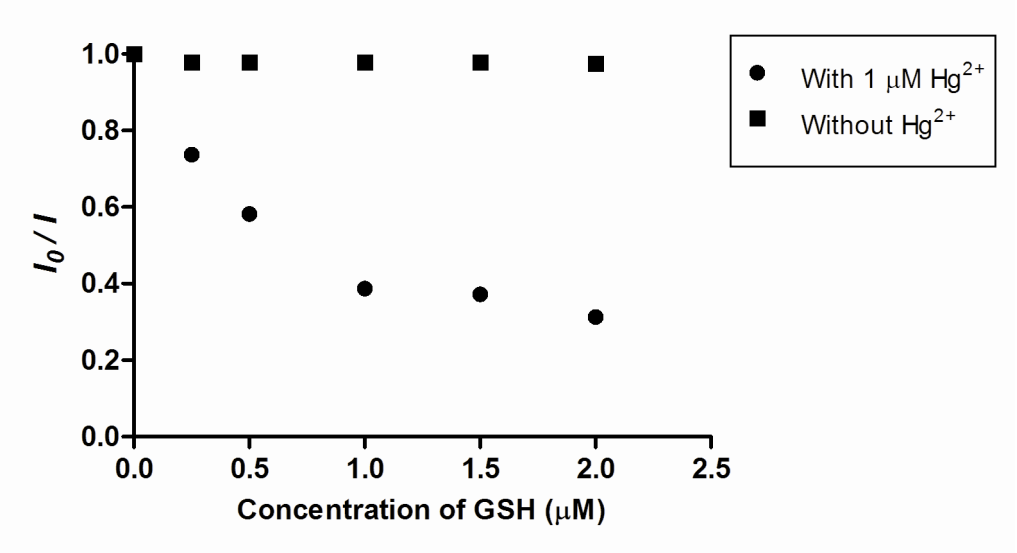

Fig. S12 Emission spectrum of the **1**/G-quadruplex/Hg^{2+} ensemble ([**1**] = 1 μM, [PS2.M] = 5 μM, [Hg^{2+}] = 1 μM) in buffered solution (20 mM Tris, pH 7.0) containing ss DNA (5 μM) and ct DNA (5 μM) in the presence of increasing concentrations of Cys (0, 0.1, 0.3, 0.5, 1, 1.5 and 2 μM). B) Luminescence response of three-component ensemble at λ = 583 nm *vs.* Cys concentration. Inset: linear plot of the change in luminescence intensity at λ = 583 nm *vs.* Cys concentration.

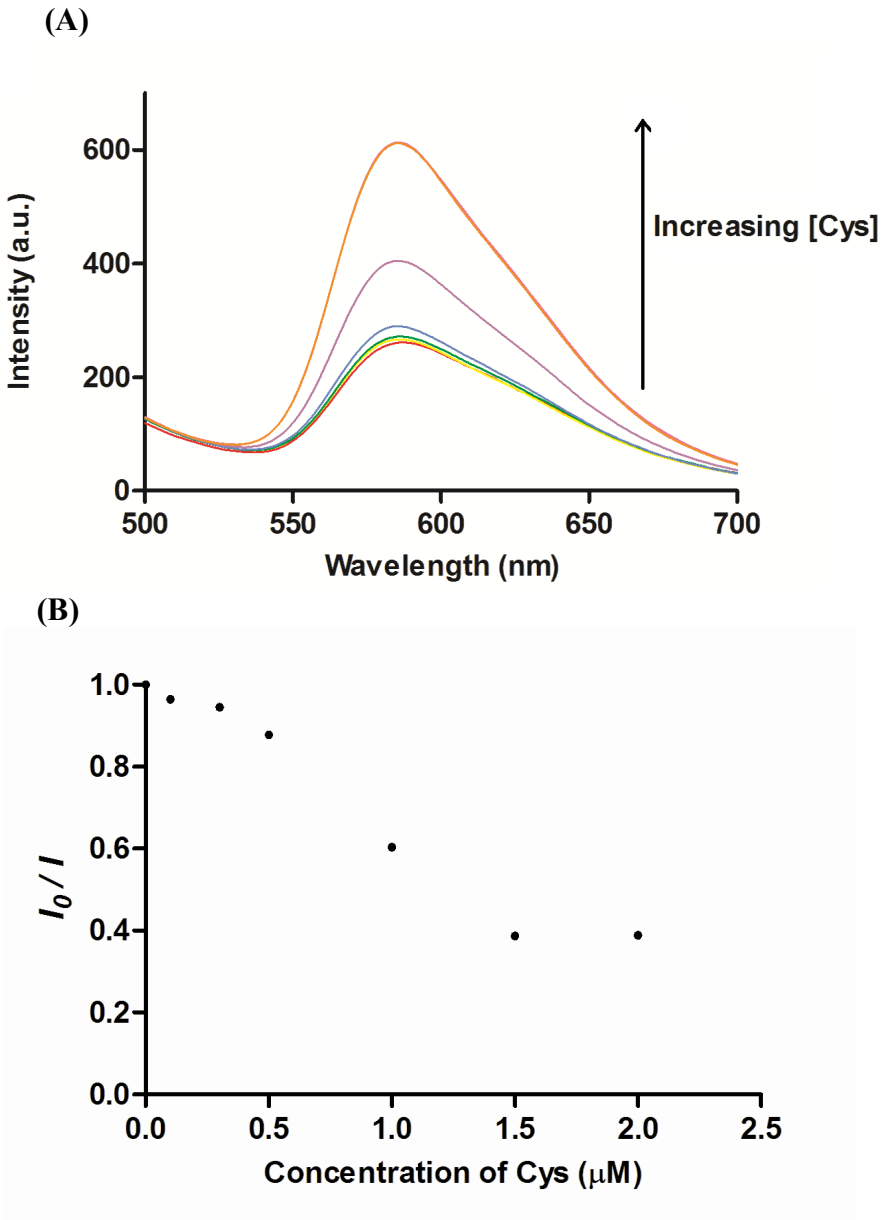

Fig. S13 Emission spectrum of the **1**/G-quadruplex/Hg^{2+} ensemble ([**1**] = 1 μM, [PS2.M] = 5 μM, [Hg^{2+}] = 1 μM) in buffered solution (20 mM Tris, pH 7.0) containing ss DNA (5 μM) and ct DNA (5 μM) in the presence of increasing concentrations of GSH (0, 0.1, 0.3, 1, 1.5, 2, 2.5 and 3 μM). B) Luminescence response of three-component ensemble at λ = 583 nm *vs.* GSH concentration. Inset: linear plot of the change in luminescence intensity at λ = 583 nm *vs.* GSH concentration.

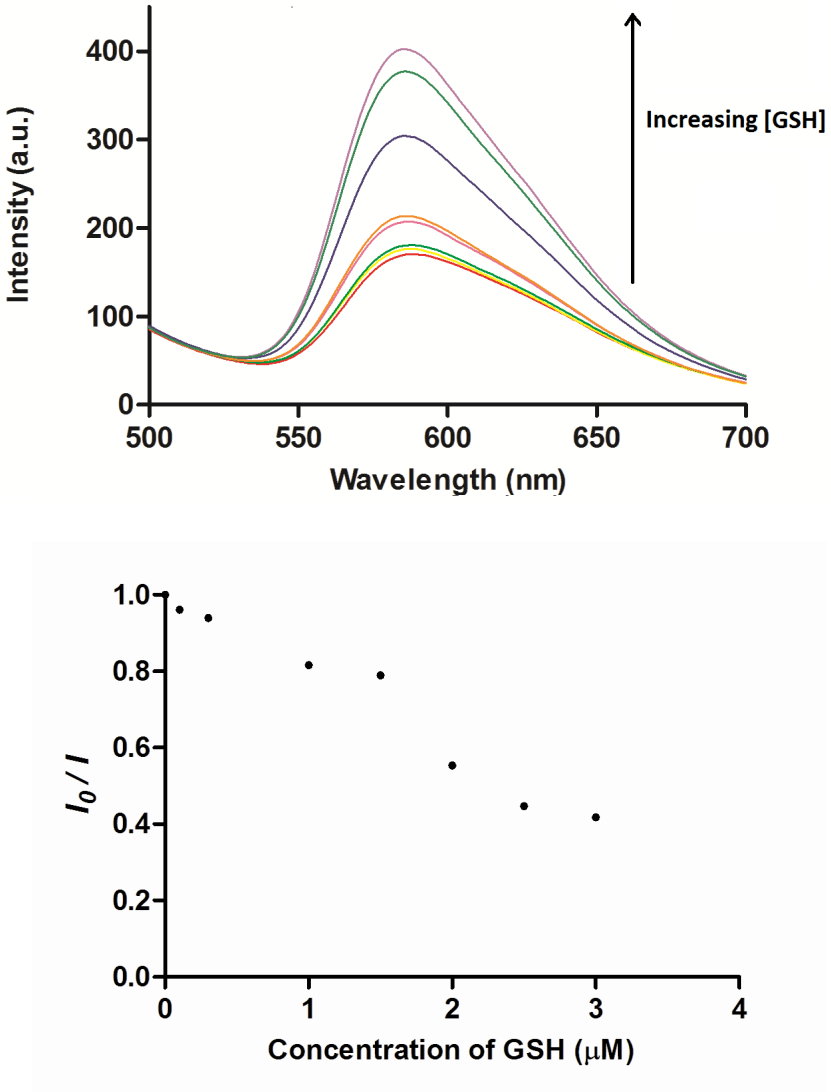

Fig. S14 Emission spectrum of the **1**/G-quadruplex/Hg^{2+} ensemble ([**1**] = 1 μM, [PS2.M] = 5 μM, [Hg^{2+}] = 500 μM) in 50-fold diluted urine sample in the presence of increasing concentrations of Cys (0, 100, 300, 400, 500, 600, 700, 800, 900, 1000, 1200 and 1500 μM). B) Stern-Volmer plot of the three-component ensemble at λ = 583 nm *vs.* Cys concentration.

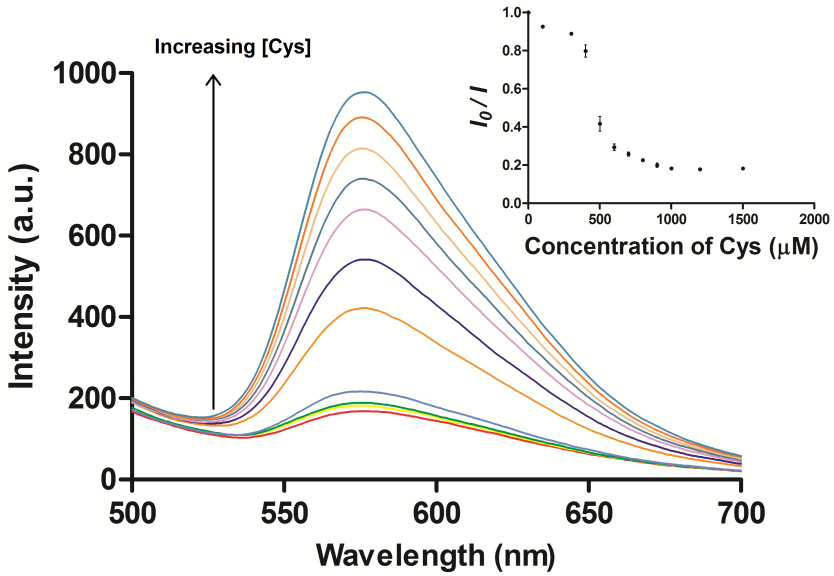

Fig. S15 Emission spectrum of the **1**/G-quadruplex/Hg^{2+} ensemble ([**1**] = 1 μM, [PS2.M] = 5 μM, [Hg^{2+}] = 500 μM) in 50-fold diluted urine sample in the presence of increasing concentrations of GSH (0, 100, 200, 300, 400, 500, 600, 700, 800, 900, 1000, and 1200 μM). B) Stern-Volmer plot of the three-component ensemble at λ = 583 nm *vs.* GSH concentration.

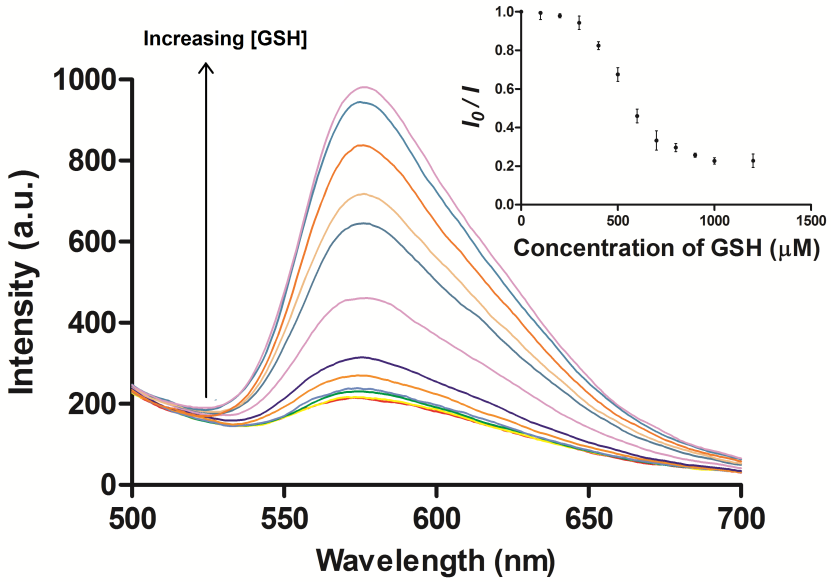

Table S1. Photophyiscal properties of complex **1** in CH_3CN at 298K.

Complex	UV/vis absorption	Emission	
	λ_{abs} [nm] (ε [$dm^3mol^{-1}cm^{-1}$])	λ_{em} [nm] (τ [μs])	Quantum yield Φ
1	267 (sh), 280 (3.6×10^4), 348 (sh), 429 (5.9×10^3)	583 (4.31)	0.27

Table S2. Comparison of detection limit and range for some recently reported analytical techniques for biothiols. References refer to those in the supporting information.

Method	*Detection limit*	*Range*	*Analyte*	*Ref.*
CdTe/CdSe quantum dots	0.1 μM	0.6–20 μM	GSH only	4
CdTe quantum dots	0.6 μM (Cys) 0.1 μM (GSH)	2–20 μM (Cys) 0.6–20 μM (GSH)	Cys, GSH	5
A thiol specific fluorescent probe	50 nM (Cys) 100 nM (Hcy) 53 nM (GSH)	0–350 nM (GSH) N.A. (Cys and Hcy)	Cys, GSH and Hcy	6
DNA/thiazole orange/Hg^{2+} ensemble	5.1 nM	Tunable	Cys only	7
Hg^{2+} based molecular beacon	4.2 nM (Cys) 4.1 nM (GSH)	4 nM–200 nM (Cys and GSH)	Cys and GSH	8
Fluorescent silver nanoclusters based on oligonucleotide	4 nM (Cys) 0.2 nM (Hcy) 4 nM (GSH)	8–100 nM (Cys) 0.6–2 μM (Hcy) 8–100 nM (GSH)	Cys, Hcy and GSH	9
Hg^{2+}/carbon nanodots	4.9 nM (Cys) 6.1 nM (Hcy) 8.5 nM (GSH)	10 nM–5 μM (Cys, Hcy and GSH)	Cys, Hcy and GSH	10
Method in this study	5 nM (Cys) 10 nM (GSH)	Tunable	Cys and GSH	

References

1. G. A. Crosby and J. N. Demas, *J. Phys. Chem.,* 1971, **75**, 991–1024.
2. M. S. Lowry, W. R. Hudson, R. A. Jr. Pascal and S. Bernhard, *J. Am. Chem. Soc.,* 2004, **126**, 14129–14135.
3. C. O. Dietrich-Buchecker, P. A. Marnot, J.-P. Sauvage, J. R. Kirchhoff and D. R. McMillin, *J. Chem. Soc. Chem. Commun.*, 1983, 513–515.
4. Y. Zhang, Y. Li and X. Yan, *Anal. Chem*., 2009, **81,** 5001–5007.
5. B. Han, J. Yuan and E. Wang, *Anal. Chem*., 2009, **81**, 5569–5573.
6. X. Chen, S. K. Ko, M. J. Kim, I. Shin and J. Yoon, *Chem. Commun.*, 2010, **46**, 2751–2753.

7. F. Pu, Z. Huang, J. Ren and X. Qu, *Anal. Chem.*, 2010, **82**, 8211–8216.
8. H. Xu and M. Hepel, *Anal. Chem.*, 2011, **83**, 813-819.
9. B. Han and E. Wang, *Biosens. Bioelectron*., 2011, **26**, 2585–2589.
10. L. Zhou, Y. Lin, Z. Huang, J. Ren and X. Qu, *Chem Commun.*, 2012, **48**, 1147–1149